5th IAA Conference on Space Situational Awareness (ICSSA)

Tres Cantos - Madrid, Spain

IAA-ICSSA-26-xxxx
THERMO-OPTICAL CHARACTERIZATION AND QUALIFICATION OF A SPACE SITUATIONAL AWARENESS (SSA) PAYLOAD

Ian Porto[1], **Marissa Myhre**[1], **Vithurshan Suthakar**[1], **Regina S.K. Lee**[1]
[1] York University, 4700 Keele St, Toronto, Ontario, Canada, +1 416 736-2100, ianporto@yorku.ca, reginal@yorku.ca*

Keywords: *Space Situational Awareness (SSA), Commercial off-the-Shelf (COTS) Components, Thermo-Optical Characterization, Environmental Qualification, Optical Payload*

Abstract

Operating in the congested, contested, and competitive space environment has never been more challenging in the history of space exploration. Consequently, space situational awareness (SSA), which involves monitoring and characterizing resident space objects (RSOs), has been identified by the research community as a top priority for space activities globally. To address limitations in SSA data acquisition, we developed a commercial off-the-shelf (COTS) wide field-of-view (WFOV) optical sensor. In this study, we present a Technology Readiness Level (TRL) 7 payload comprising a 4.2-megapixel sCMOS sensor and a lens with a $29.7^\circ \times 29.7^\circ$ field of view, which has flown three times on stratospheric balloon missions with the Canadian Space Agency and the Centre National d'Études Spatiales.

To prepare for its upcoming orbital launch on UPMSAT-4, the payload underwent environmental characterization. While initially rated for 10 °C to 40 °C at standard pressure, previous stratospheric missions demonstrated operation at temperatures down to -10 °C. We conducted the thermal vacuum (TVAC) qualification test for the low Earth orbit environment, qualifying the payload for survival temperatures ranging from -60 °C to 60 °C and operational temperatures from -40 °C to 40 °C. As a result of these tests, we have verified that the payload meets the environmental requirements for UPMSAT-4. These tests also characterized the payload's optical parameters. Sensor readout noise was quantified via dark current tests. A 1951 USAF resolution test chart was used to quantify the optical residuals in the lens. Using the USAF target, we found the system's spatial resolution degraded to a minimum of 2.25 line pairs/mm at the temperature extremes. Dark current characterization yielded mean signal values (Digital Number, DN) of 97.99 at ranges of 20 to 40 °C, 98.42 at ranges from 40 to 60 °C, and 95.27 at ranges from -60 to -40 °C. Successful qualification of the UPMSAT-4 mission profile advances the payload to TRL 8; furthermore, the thermal-optical characterization provides the necessary baselines for future on-orbit data calibration.

1. Introduction

The proliferation of Resident Space Objects (RSOs) in Low Earth Orbit (LEO) has transformed the orbital domain into an environment that is increasingly congested, contested, and competitive [1]. To ensure the safety and sustainability of operations within this domain, Space Situational Awareness (SSA) has been identified by the global research and defence communities as a critical priority [2]. While traditional ground-based radar and optical systems provide the backbone of current catalogue maintenance, they suffer from inherent geographic limitations, weather-dependent duty cycles, and the inability to continuously track objects across all orbital regimes [3].

Space-based optical sensors offer a compelling solution to these coverage gaps, providing persistent, weather-independent observation capabilities. However, the prohibitive cost and development timelines of heritage space-grade hardware have historically limited the deployment of large-scale space-based SSA constellations. Consequently, the integration of Commercial Off-The-Shelf (COTS) star tracker-class cameras has emerged as a viable and cost-effective augmentation for opportunistic SSA [4].

This paper presents the environmental qualification and optical characterization of a COTS-based Wide Field-of-View (WFOV) imaging system developed at York University. The payload, selected for the upcoming UPMSAT-4 mission, features a 4.2-megapixel sCMOS sensor coupled with high-throughput optics. The system design has previously achieved Technology Readiness Level (TRL) 7 through three successful stratospheric balloon campaigns aboard the RSONAR missions (CSA/CNES) [5, 6, 7, 8]. However, the transition from stratospheric to orbital applications requires rigorous validation against the harsh thermal-vacuum conditions of LEO.

In this paper, we detail the Thermal Vacuum (TVAC) campaign designed to verify the payload's survival limits ($\pm 60^{\circ}$C) and operational performance ($\pm 40^{\circ}$C), derived from the UPMSAT-4 mission profile and NASA General Environmental Verification Standard qualification margins [9]. This qualification effort specifically targets the validation of COTS thermo-optical stability beyond standard industrial ratings, ensuring the sensor's suitability for the thermal environment of the nanosatellite bus.

2. Instrument Overview and Test Configuration

2.1. Payload Description

The payload under qualification is the York University Multi-Use Star Tracker (YU MUST), designed to provide low-cost, wide-field SSA data. The core imaging element is a COTS PCO Edge Panda 4.2 scientific CMOS camera [10], selected for its high quantum efficiency and low readout noise. This sensor is coupled with a Zeiss Dimension 2/25 high-speed lens ($f/2$, 25 mm focal length) [11], providing a $29.7^{\circ} \times 29.7^{\circ}$ full-angle field of view. The optical characteristics are provided in Table 1.

The design has previously achieved Technology Readiness Level (TRL) 7 through three successful stratospheric balloon flights aboard the RSONAR missions on the STRATOS-Science Balloon campaigns in 2022, 2023, and 2025 [12]. However, the transition to an orbital environment requires rigorous testing and characterization of the COTS instrument's intrinsic thermal behaviour. Unlike space-grade hardware, the thermo-optical stability and thermal noise characteristics of COTS sensors lack manufacturer specifications in vacuum conditions. Consequently, this qualification study prioritizes the characterization of the standalone camera's optical focus shift and dark

Table 1: Optical Characteristics of Payload

Parameter	Value
Aperture diameter	12.5 mm
Focal length	25 mm
Focal Ratio	f/2
Full-Angle Field of View	$29.7^\circ \times 29.7^\circ$
Lens transmission	0.94
Window transmission	0.98
Bit depth	16 bits
Exposure time	10 ms
Effective quantum efficiency (at 550 nm)	78%

current performance expected in LEO operations. Establishing these thermo-optical baselines is a critical prerequisite for finalizing the flight thermal control system and interface design for the YU MUST payload onboard the UPMSAT-4 mission.

2.2. TVAC & Optical Target Setup

Testing was performed at the Centre for Research in Earth & Space Science Thermal Vacuum facility, capable of maintaining high-vacuum conditions in the range of 1×10^{-5} to 1×10^{-6} Torr.

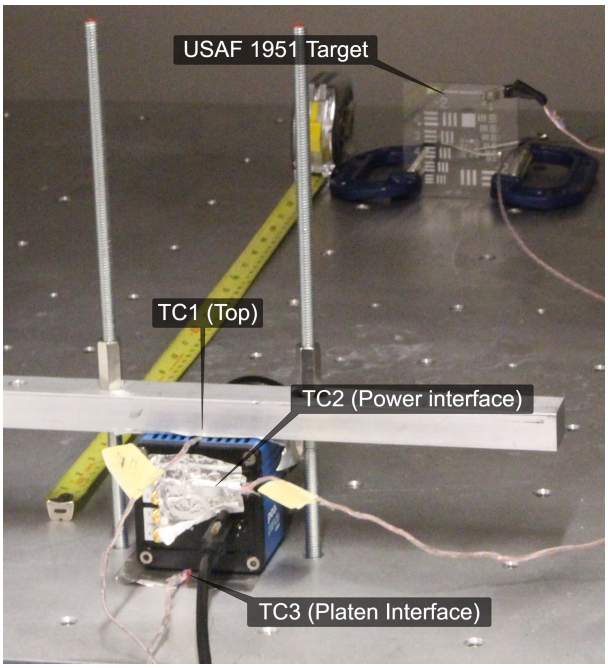

Figure 1: Image of Payload setup within the TVAC

To enable in-situ optical characterization, the payload was oriented with the lens facing the chamber interior. A 1951 USAF resolution test chart [13] was mounted and aligned with the optical axis at a working distance of 70 cm from the sensor. To illuminate the target, a broad-spectrum light source was positioned outside the chamber's rear viewport, flooding the shroud interior with diffuse white light. The payload was

mechanically secured to the chamber's thermal platen using a conductive clamping interface, as shown in Figure 1.

Thermal telemetry was acquired via a combination of external and internal sensors. Three external Type-T thermocouples monitored the test interface: (TC1) at the top clamp interface, (TC2) at the external power connector, and (TC3) at the platen interface, shown in Figure 1. Internal payload temperatures were monitored via the camera's housekeeping telemetry, which provides readings for the sCMOS sensor, the internal power board, and the FPGA [10]. An external computer automated image acquisition and telemetry logging at a rate of 1 Hz.

2.2.1. Temperature

The profile consisted of a single cycle: starting with a cold survival soak ($-60°$C), followed by the cold operational plateau ($-40°$C), the hot operational plateau ($+40°$C), and finally the hot survival soak ($+60°$C).

These target temperatures were derived from the UPMSAT-4 mission thermal analysis with specific reference to industry standards. The operational limits ($\pm 40°$C) bound the typical reliable range for industrial-grade COTS electronics [14]. The survival limits ($\pm 60°$C) incorporate a $20°$C qualification margin beyond the operational envelope, satisfying and exceeding the minimum $10°$C margin recommended by the General Environmental Verification Standard (GEVS) [9]. In Figure 2, these temperatures are outlined, as well as the planned operational state of the camera.

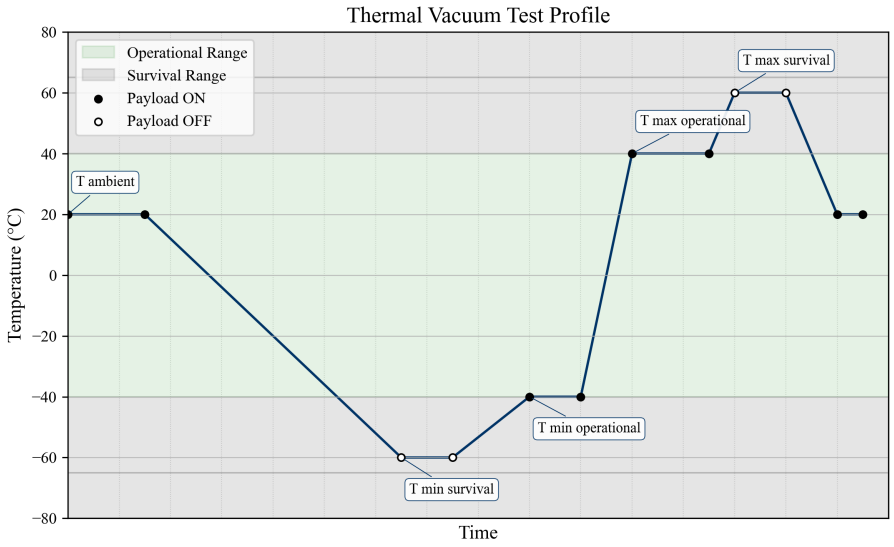

Figure 2: Planned Thermal profile

2.2.2. Sensor Characterization (Dark Current)

To quantify the thermal noise floor of the sCMOS sensor, dark current data were collected at each operational temperature plateau. To achieve a calibrated dark environment, the target illumination was extinguished. Additionally, the viewport was physically covered with an opaque material to prevent stray laboratory light from entering the chamber and reflecting off the shroud walls into the sensor aperture. A series of dark frames were captured at steady-state temperatures to calculate the mean Digital Number (DN), verifying the sensor's noise performance against mission requirements.

2.2.3. Optical Residuals (USAF 1951)

Spatial resolution and focus stability were assessed using the USAF 1951 resolution test chart mounted inside the chamber. At various points during the TVAC test, including the Cold Operational ($-40°$C) and Hot Operational ($+40°$C) plateaus as well as the slew between them, the target was illuminated, and images and temperatures were recorded.

Images of the chart were captured to quantify the limiting resolution degradation caused by the coefficient of thermal expansion mismatch between the lens elements and the sensor body. The success criterion for this test was that the system maintain a minimum limiting resolution sufficient for RSO centroiding and attitude determination algorithms and that the lens assembly exhibit no permanent visual deformities after thermal cycling.

3. Results

3.1. Thermal Execution

The thermal vacuum qualification profile is presented in Figure 3. The test campaign yielded three distinct datasets corresponding to the operational phases. In Figure 3 we can see the temperatures of interest, divided into two colour profiles: survival in grey and operational in green. Figure 3 is divided into three sections, each corresponding to one of the following phases denoted at the top of the figure:

- **Phase 1:** The payload temperature did not reach required thermal temperatures. Platen temperature was unable to remain at the required $-60°C$.
- **Phase 2:** The payload successfully completed the hot operational soak at $+40°C$ and the survival soak at $+60°C$.
- **Phase 3:** Following a chamber break to fix payload contact with the platen, the payload achieved the target survival temperature of $-60°C$ and stabilized at the $-40°C$ operational plateau.

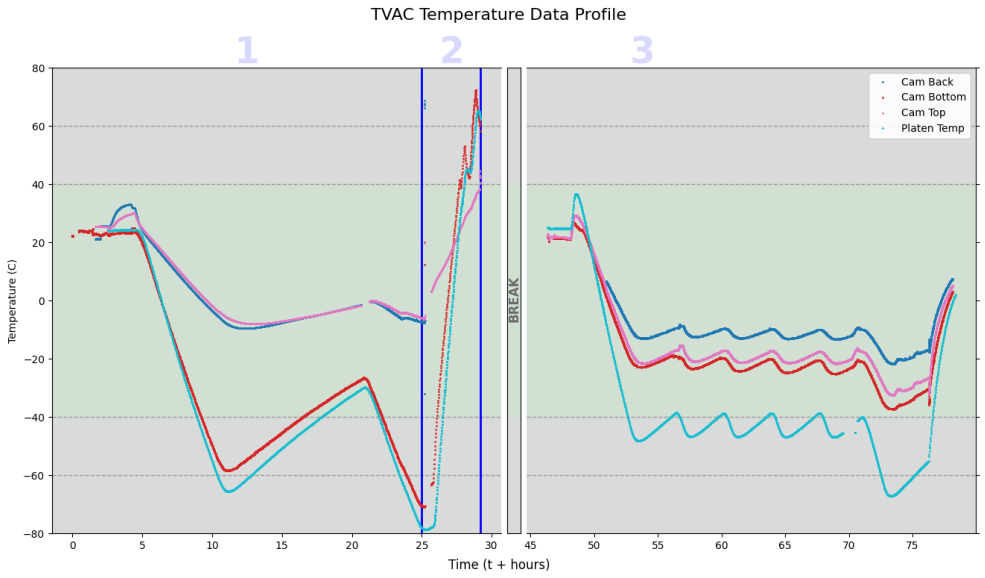

Figure 3: Measured temperature profile, showing the initial cold attempt (Phase I), the hot cycles (Phase II), and the final successful cold soak (Phase III).

3.2. Dark Current Characterization

Throughout the test, 2280 dark current images were captured; payload imaging parameters are outlined in Table 1. Their data was divided into $20^{\circ}C$ temperature ranges to quantify the sensor's thermal noise floor across the full range.

The contrast-stretched Master Dark Image (Figure 4) confirms the absence of hot pixels or localized defects; however, faint column-wise banding and edge shading are visible. This low-level fixed-pattern noise is a well-documented artifact of the sCMOS column-parallel analogue-to-digital converter readout architectures [15]. Because each column utilizes its own dedicated readout circuitry, slight variations in amplifier gain and offset naturally manifest as vertical stripes. The statistical variations of this dark current across the tested temperature ranges are detailed in Table 2.

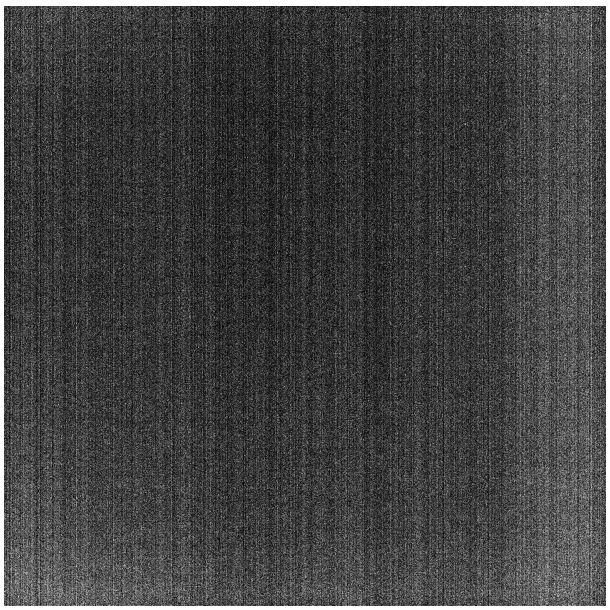

Figure 4: Master Dark Image (Enhanced for noise pattern visibility)

Dark current statistics were calculated for steady-state temperature bins (Table 2). In the nominal operational range ($-40^{\circ}C$ to $+40^{\circ}C$), the mean signal ranged from 96.89 Digital Number (DN) to 97.99 DN. The maximum noise floor of 98.42 DN was recorded during the $+60^{\circ}C$ survival soak.

Table 2: Dark Current Statistics vs. Temperature

Temperature Range ($^{\circ}C$)	Samples	Mean DN	Std. Dev
-60 to -40	24	95.27	0.33
-40 to -20	130	96.89	0.20
-20 to 0	103	97.34	0.13
0 to 20	29	97.40	0.14
20 to 40	120	97.99	0.33
40 to 60	175	98.42	0.15

3.3. Spatial Resolution Degradation

During the test, 7,589 images of a USAF 1951 target were captured. Figure 5 presents the limiting resolution measured via the USAF 1951 target. At ambient and hot operational temperatures ($> 20°C$), the system resolved approximately 3.4-3.5 lp/mm. As the temperature decreased below $0°C$, the resolution stabilized at 2.3 lp/mm at the $-40°C$ operational limit. The step-like transitions observed in the resolution data between $-40°C$ and $0°C$ are an artifact of the discrete sampling intervals defined in the test plan, rather than an abrupt physical shift in the optical performance.

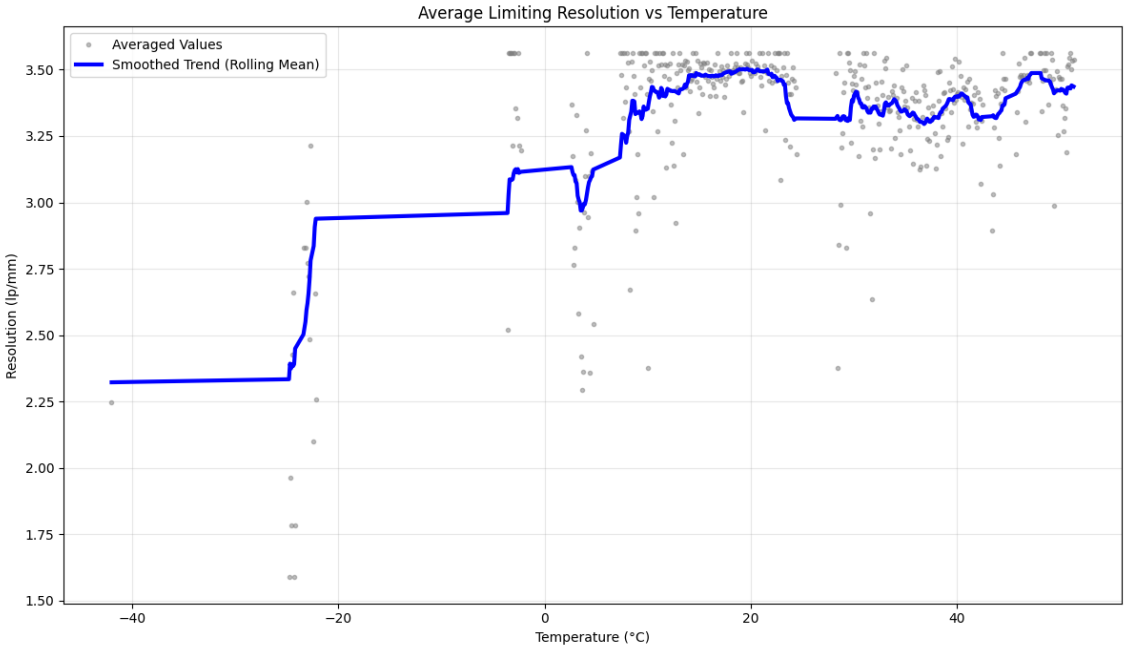

Figure 5: Limiting Resolution (lp/mm) vs. Temperature.

3.3.1. Spatial Resolution Sample Image

To assess spatial resolution and focus stability in real-time, the payload captured images of a standard USAF 1951 resolution test chart mounted directly inside the TVAC chamber at a fixed working distance. The target was illuminated by a broad-spectrum light source positioned outside the chamber's rear viewport. This external arrangement provided the uniform, diffuse white light necessary to mitigate stray specular reflections within the shroud, ensuring an accurate quantification of the optical residuals of the lens at various temperature plateaus.

Figure 6 provides a direct visual comparison of the target at two focal extremes. Figure 6(a) demonstrates the baseline focus achieved at ambient temperature. In this state, the finer groupings of the test chart, specifically the distinct separation between the horizontal and vertical three-bar elements, are clearly resolved. In contrast, Figure 6(b) illustrates the thermo-optical defocus experienced at $-20°C$, which shows distinct blurring of the horizontal and vertical bar elements, especially in the 0 and 1 groups.

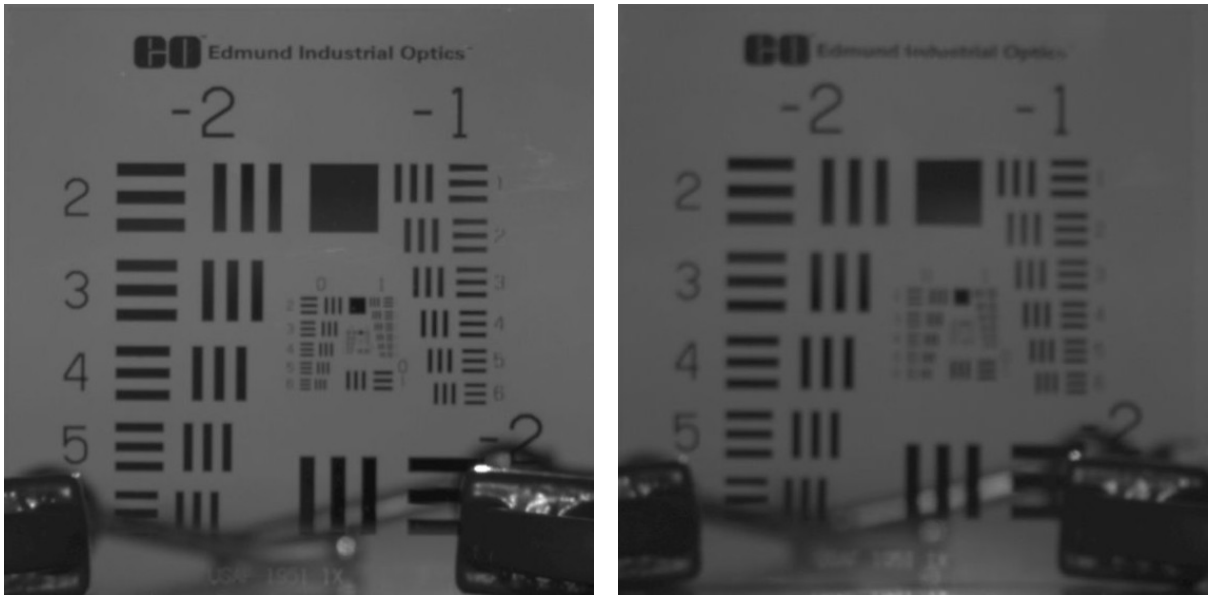

(a) (b)

Figure 6: Visual comparison of the USAF 1951 test chart focus stability at (a) ambient temperature and (b) -20°C.

4. Discussion and Lessons Learned

4.1. Interface Sensitivity in Vacuum

The telemetry from **Phase 1** (Figure 3) reveals a significant thermal decoupling, evidenced by a $\sim 60^{\circ}C$ gradient between the payload baseplate (TC3) and the top (TC1) and power interface (TC2) of the payload. This is attributed to three compounding factors.

First, the absence of a flight-specific thermal baseplate reduced the conductive contact area between the payload and the platen. Second, the interface thermocouple (TC3) created a mechanical standoff gap, effectively breaking the primary thermal path as shown in Figure 7. Finally, a reduction in the facility's platen gas pressure constrained the available cooling capacity, preventing the heat sink from maintaining the target temperature under the payload's thermal load. This facility anomaly was rectified in Phase 3, enabling the system to successfully reach the $-60^{\circ}C$ survival floor.

Phase 2 (Hot Cycles) was executed successfully despite these interface limitations. Since the payload generates internal heat, the radiative and conductive resistance worked in favour of the hot case, allowing the sensor to easily reach the $+40^{\circ}C$ operational and $+60^{\circ}C$ survival targets. Following Phase 2, the chamber was vented to allow for payload re-seating. The interface thermocouple (TC3) was relocated to the indium thermal interface sheet to eliminate the mechanical gap.

Phase 3 (Cold Cycles) demonstrated the success of this remediation. With the conductive path restored and facility pressure normalized, the payload successfully achieved the $-60^{\circ}C$ survival soak and the $-40^{\circ}C$ operational plateau, validating the necessity of high-fidelity interface integration for vacuum operations.

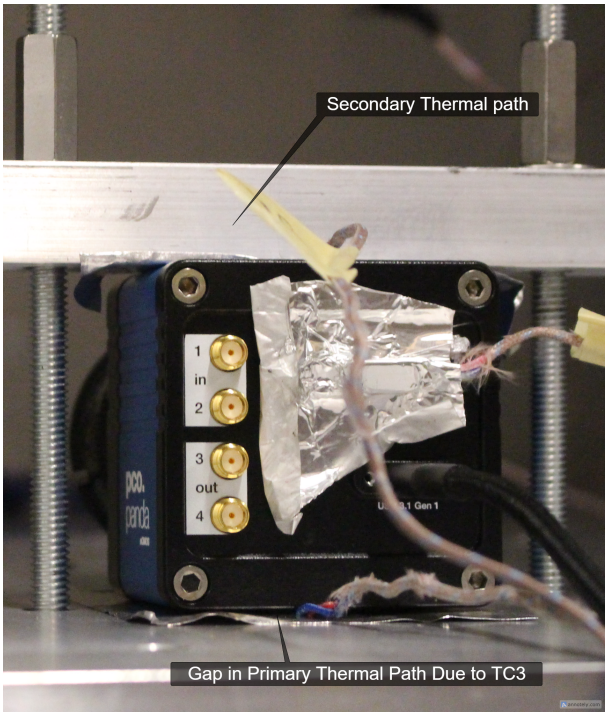

Figure 7: Gap in Thermal Path Caused by TC3

4.2. Thermo-Optical Stability

The optical data (Figure 5) indicates a thermally induced focus shift. The degradation from 3.5 lp/mm to 2.3 lp/mm at cold temperatures is consistent with a coefficient of thermal expansion mismatch between the aluminium lens barrel and the sensor structure. While the resolution degraded, it remained within the limits required for the YU MUST mission objectives.

However, characterizing this degradation is significant for the payload's operational viability. In Space Situational Awareness (SSA), accurate orbit determination relies on the sub-pixel centroiding of RSOs. The observed resolution drop at cold extremes represents a spatial broadening of imaged point sources. This thermo-optical behaviour was fully expected for a COTS objective lens operating in a vacuum environment without active thermal control. Similar thermal defocusing trends have been reported in other nanosatellite missions utilizing COTS optics [16]. For the UPMSAT-4 mission, this means that stars and RSOs imaged will span more pixels, which increases the importance of a robust centroid method.

The operating temperature range for the payload within the UPMSAT-4 bus is expected to be -10°C to 40°C. Therefore, the successful spatial resolution retention across the broader -40 ℃ to 40 ℃ operational plateau provides a robust thermal margin for flight.

Regarding the sensor's thermal noise profile, the calculated standard deviation shown in Table 2 serves as a metric for the temperature stability of the sensor's average dark level. For SSA missions, this stability is critical; any significant thermal instability during an image sequence could introduce artifacts that mimic or obscure RSOs [17]. The low variance observed confirms that the sensor maintains a consistent noise floor, ensuring that observations remain reliable across a wide range of operational temperatures.

5. Conclusion

In this study, we presented the thermal-vacuum qualification of the York University Multi-Use Star Tracker, validating a low-cost, COTS-based imaging system for space situational awareness. Through a rigorous test campaign, the payload demonstrated survival across the full $\pm 60^{\circ}C$ envelope and nominal operation within the $\pm 40^{\circ}C$ range. This wide operational plateau provides a robust thermal margin well beyond the anticipated -10°C to 40°C operating environment of the spacecraft bus, satisfying all requirements for the UPMSAT-4 mission and advancing the system to TRL 8.

Beyond verification, the campaign provided critical insights into the integration of commercial hardware for space applications. The initial thermal decoupling observed in Phase 1 serves as a significant case study, highlighting that for passively cooled COTS instruments, the fidelity of the vacuum mechanical interface is the primary determinant of survival. Following interface optimization, the payload exhibited robust thermal stability.

Future work will focus on integrating the qualified flight model onto the UPMSAT-4 bus with our partners at Universidad Politécnica de Madrid and finalizing the payload's thermal interface. Utilizing this thermo-optical dataset, we will develop a comprehensive master-dark calibration library, which will be implemented directly into the mission's data processing pipeline to further optimize RSO detection.

Optical characterization established the necessary baselines for on-orbit operations. A thermally induced focus shift was quantified, degrading limiting resolution from 3.5 lp/mm at ambient to 2.3 lp/mm at $-40^{\circ}C$. This spatial broadening was fully expected for COTS optics and aligns closely with thermo-optical behaviours reported in similar nanosatellite missions [16]. Despite this shift, the system maintains sufficient acuity for RSO centroiding. Furthermore, the sCMOS sensor demonstrated exceptional noise stability, with dark current varying by less than 3 DN across the operational range. These results qualify the current flight model and provide a verified thermo-optical dataset that will enable high-fidelity calibration of the YU MUST payload.

Acknowledgments

This research was funded by the Natural Sciences and Engineering Research Council of Canada (NSERC) Discovery Grant; by the Department of National Defence (Canada) and NSERC through the DND/NSERC Discovery Grant Supplement; and by the Canadian Space Agency (CSA) through the Flights and Fieldwork for the Advancement of Science and Technology (FAST) program.

References

[1] Department of Defense, "National Security Space Strategy: Unclassified Summary." Office of the Secretary of Defense, 2011.

[2] ESA Space Debris Office, "ESA's Annual Space Environment Report," Tech. Rep. Issue 9.1, GEN-DB-LOG-00288-OPS-SD, European Space Operations Centre (ESOC), Darmstadt, Germany, Oct 2025. Available: `https://www.sdo.esoc.esa.int/publications/Space_Environment_Report_I9R1_20251021.pdf`.

[3] A. Bloom, J. Wysack, J. D. Griesbach, and A. Lawitzke, "Space and ground-based sda sensor performance comparisons," in *Advanced Maui Optical and Space Surveillance Technologies Conference*, pp. 1–11, Maui Economic Development Board Maui, HW, 2022.

[4] G. Chianelli, P. Kunalakantha, M. Myhre, and R. S. K. Lee, "A dual-purpose camera for attitude determination and resident space object detection on a stratospheric balloon," *Sensors*, vol. 24, no. 1, 2024.
[5] P. Kunalakantha, A. V. Baires, S. Dave, R. Clark, G. Chianelli, and R. S. K. Lee, "Stratospheric night sky imaging payload for space situational awareness (ssa)," *Sensors*, vol. 23, no. 14, 2023.
[6] V. Suthakar, A. A. Sanvido, R. Qashoa, and R. S. Lee, "Comparative analysis of resident space object (rso) detection methods," *Sensors*, vol. 23, no. 24, p. 9668, 2023.
[7] V. Suthakar, I. Porto, M. Myhre, A. A. Sanvido, R. Clark, and R. S. Lee, "Rsonar: Data-driven evaluation of dual-use star tracker for stratospheric space situational awareness (ssa)," *Sensors*, vol. 26, no. 1, p. 179, 2025.
[8] R. Qashoa, V. Suthakar, G. Chianelli, P. Kunalakantha, and R. S. K. Lee, "Technology demonstration of space situational awareness (ssa) mission on stratospheric balloon platform," *Remote Sensing*, vol. 16, no. 5, 2024.
[9] NASA Goddard Space Flight Center, "General Environmental Verification Standard (GEVS) for GSFC Flight Programs and Projects," Tech. Rep. GSFC-STD-7000B, NASA, Greenbelt, MD, 2021. Section 2.6.
[10] PCO AG, *pco.panda User Manual*. PCO AG, Donaupark 11, 93309 Kelheim, Germany, v1.00 ed., July 2018. Available at `www.pco.de`.
[11] Carl Zeiss AG, *ZEISS Dimension 2/25 Datasheet*. Carl Zeiss AG, Oberkochen, Germany, 12 2024. Subject to change.
[12] Canadian Space Agency, "About STRATOS, the CSA's stratospheric balloon program," 2025.
[13] Edmund Optics, "1951 USAF glass slide resolution targets." `https://www.edmundoptics.es/f/1951-usaf-glass-slide-resolution-targets/12064/`. Accessed: 2024-05-22.
[14] J. R. Wertz and W. J. Larson, *Space Mission Analysis and Design*. Torrance, CA: Microcosm Press, 3rd ed., 1999.
[15] Z. Zhang, Y. Wang, R. Piestun, and Z. li Huang, "Characterizing and correcting camera noise in back-illuminated scmos cameras," *Opt. Express*, vol. 29, pp. 6668–6690, Mar 2021.
[16] D. Garranzo, A. Núñez, H. Laguna, T. Belenguer, E. De Miguel, M. Cebollero, S. Ibarmia, and C. Martínez, "Apis: the miniaturized earth observation camera on-board optos cubesat," *Journal of Applied Remote Sensing*, vol. 13, no. 3, pp. 032502–032502, 2019.
[17] F. S. Ribeiro, P. J. Garcia, M. Silva, and J. S. Cardoso, "Space imaging point source detection and characterization," *IEEE Access*, vol. 12, pp. 90442–90460, 2024.